Open Access

Catalysis Research

LIDSEN Publishing Inc.

Original Research

Hierarchical MFI Zeolite Catalysts: How to Determine Their Textural Properties?-A Comparative Study

Anne Galarneau [1,*], Lucie Desmurs [1], Cyril Vaulot [2,3], Habiba Nouali [2,3], Benedicte Lebeau [2,3], T. Jean Daou [2,3], Vasile Hulea [1], Claudia Cammarano [1], Isabelle Batonneau-Gener [4], Alexander Sachse [4]

1. Institut Charles Gerhardt Montpellier, ICGM, Univ Montpellier, CNRS, ENSCM, Montpellier, France; E-Mails: anne.galarneau@enscm.fr; lucie.desmurs@enscm.fr; vasile.hulea@enscm.fr; claudia.cammarano@enscm.fr
2. Université de Haute Alsace (UHA), CNRS, IS2M UMR 7361, F-68100, Mulhouse, France; E-Mails: cyril.vaulot@uha.fr; habiba.nouali@uha.fr; benedicte.lebeau@uha.fr; jean.daou@uha.fr
3. Université de Strasbourg, F-67000 Strasbourg, France
4. Institut de Chimie des Milieux et Matériaux de Poitiers (IC2MP), Université de Poitiers-UMR 7285 CNRS, UFR SFA, Bat. B27, 4 rue Michel Brunet, TSA 51106, 86073 Poitiers, Cedex 9, France; E-Mails: isabelle.gener@univ-poitiers.fr; alexander.sachse@univ-poitiers.fr

* **Correspondence:** Anne Galarneau; E-Mail: anne.galarneau@enscm.fr

Academic Editor: Angela Martins

Special Issue: Zeolite Materials and Catalysis

Catalysis Research
2022, volume 2, issue 2
doi:10.21926/cr.2202009

Received: January 26, 2022
Accepted: March 24, 2022
Published: April 14, 2022

Abstract

It is important to elucidate the role of the surface areas and pore volumes of hierarchical zeolites to understand their behavior as catalysts. Micro-and mesopore surface areas and volumes of the hierarchical MFI (Mobil Five zeolites) were assessed following several methods: (*i*) N_2 adsorption at 77 K using classical and corrected *t*-plot analyses methods, (*ii*) pre-adsorption of *n*-nonane was followed by the study of the N_2 adsorption at 77 K, and (*iii*) non-local-density functional theory (NLDFT) analysis using either the N_2 adsorption method at 77 K or the Ar adsorption method at 87 K. In order to assess the viability of each method,

a set of hierarchical MFI-type zeolites was prepared by different approaches: alkaline treatment (desilication), synthesis in clear solution (nanocrystals), synthesis in the presence of bifunctional organic surfactant (nanosheets), and micelle-templating assisted alkaline treatment. NLDFT methods could not be used to accurately determine the micro-and mesopore surface areas, as larger surface areas compared to those obtained using the BET equation were obtained. This overestimation is even more pronounced with Ar at 87 K. Results from the classical *t*-plot analysis performed under conditions of N_2 adsorption at 77 K for mechanical mixtures of MFI and MCM-41 revealed the underestimation of the micropore volumes and the overestimation of the mesopore surface areas. Corrections were provided for *t*-plot analysis. The results obtained using the corrected *t*-plot method were in good agreement with the results obtained using the NLDFT method in the presence of Ar at 87 K during the calculation of the micro-and mesopore volumes of hierarchical MFI-type zeolites. Micropore and mesopore surface areas calculated by the corrected *t*-plot method were in good agreement with those calculated using the *n*-nonane pre-adsorption method for the hierarchical MFI-type zeolites characterized by the presence of large zeolite domains. The NLDFT method, in the presence of Ar, can be used to assess the micro-and mesopore volumes of the hierarchical zeolites at 87 K. However, it cannot be used to determine the surface areas. The corrected *t*-plot method can be used to efficiently calculate both the volumes and surface areas.

Keywords
Mesoporous zeolite; micropore; ZSM-5; surface area; pore volume; t-plot; NLDFT; n-nonane; isotherm; textural properties

1. Introduction

Zeolites are a family of aluminosilicates that are characterized by unique textural and chemical properties. These microporous materials find applications in various industries, including oil refining and petrochemistry [1]. More than 250 zeolite structures are known. Of these, the zeolites characterized by an MFI framework (especially ZSM-5) are of particular interest in the field of acid catalysts as they can be used in the hydrocarbon conversion processes. MFI-type zeolites are used in at least 31 different industrial processes, including alkylation and isomerization. They are widely used in Fluid Catalytic Cracking (FCC) formulation, where they are used as additives to ultrastable Y zeolites to tune the yields of propylene and improve the gasoline octane number [2]. The MFI type framework is characterized by the presence of two types of intersecting channels: straight channel (with an elliptical cross-section; 0.52 × 0.56 nm) and sinusoidal channel (with quasi-circular cross-section; 0.54 × 0.56 nm). These two-channel systems are connected with each other, resulting in the formation of an intersection with a diameter of approximately 0.8 nm. The dimension imparts the shape and selective properties to the zeolite systems. Despite their unique properties, the presence of micropores in these materials often hinders the process of intracrystalline diffusion, resulting in inefficient mass transport through the extended zeolite

micropore system [3]. In other words, some of the active sites in the zeolite remain inaccessible and do not participate in the catalytic process.

It has been proposed that the diffusion path length of different types of zeolites, such as MFI, MOR, *BEA, and FAU-Y, should be shortened using various strategies to address this problem [4-18]. The strategies include (*i*) coating the zeolite crystals with a thin layer of mesoporous material [5, 6], (*ii*) using micro-/mesoporous nanocomposites with large domains for both micro-and mesoporous materials [5, 7], (*iii*) using mesoporous materials containing small zeolitic fragments in the pore walls [5, 6, 8], (*iv*) using ordered [9] or disordered [10, 11] mesoporous materials with zeolitic walls, (*v*) dispersing zeolite nanocrystals into mesoporous materials characterized by either an amorphous or a zeolitic wall [12], and (*vi*) using nanocrystals [13, 14] and nanosheets of zeolite aggregates [15]. The presence of bimodal porosity in hierarchical zeolites causes significant changes in numerous physicochemical properties of conventional zeolites. In the field of catalysis, the use of hierarchical zeolites can help in the reduction of the diffusion path length of the intact micropore domains of the zeolite and enhance the accessibility of bulky molecules (the sizes of which are greater than the sizes of the micropores). This is achieved by increasing the number of pore mouths per unit of the external surface. This allows efficient intra-particular transport, resulting in higher catalytic activities and increased selectivity and catalyst stability. These can be attributed to the reduction of secondary reactions and coking [19]. Enhanced catalytic performances of hierarchical zeolites have been reported in the literature [20-30].

The micro-and mesopore volumes and the pore size distribution of hierarchical zeolites can be assessed by analyzing the adsorption data obtained using molecular simulation techniques (such as the non-local-density functional theory (NLDFT method)) and adsorbate-adsorbent interaction models [31]. The process of N_2 sorption at 77 K is classically and generally used and accepted as the standard method for the analysis of both micropores and mesopores. However, to evaluate the micropore volumes and the pore sizes of zeolites, or more generally, of micropore-containing materials, the use of the NLDFT method applied to Ar adsorption isotherm recorded at 87 K has been highly recommended by the International Union of Pure and Applied Chemistry (IUPAC) and the International Standard Organization (ISO) in 2007 (such as ISO-15901-3) [32]. As liquid Ar is expensive, it is seldom used in research laboratories. However, new cryostats are now available, which enable the recording of Ar isotherms at 87 K using liquid N_2. NLDFT methods were used to characterize pore size distributions and pore volumes of hierarchical zeolites such as hierarchical MFI-type zeolites [4, 33-35] and hierarchical FAU-Y [9, 26, 27, 36].

The influence of the micro-/and mesopore surface areas of hierarchical zeolites in the field of catalysis and adsorption is seldom discussed. In general, only the total surface area calculated by the BET equation is discussed. The BET area (S_{BET}) classically used to characterize the textural properties of zeolites, is far from being satisfactory and does not allow the elucidation of the role of micro-and mesopore surface areas of the hierarchical materials. The *t*-plot analysis method can be used to theoretically obtain the desired values. The method was used by a few researchers to analyze hierarchical zeolites. This method has been primarily used to determine the external surface areas and micropore volumes [16, 17, 20, 37]. However, the method is complex. Results obtained by conducting computational studies revealed that the *t*-plot method underestimates the micropore volumes and overestimates the mesopore surface areas of hierarchical materials [38-40]. This was confirmed experimentally using mechanical mixtures of zeolites and MCM-41 [41-43]. The *t*-plot method was corrected to accurately calculate the micro-and mesopore

volumes and the mesopore plus external surface areas of hierarchical zeolites [41-43]. The micropore surface area was obtained by subtracting the mesopore plus external surface area from the total surface area given by the BET area (S_{BET}). As the efficiency of using S_{BET} for zeolites is under debate, we demonstrated [43] that the calculated S_{BET} value (calculated based on the Rouquerol criteria and the cross-sectional area of nitrogen (0.162 nm^2)) can be used for several zeolites. The BET area matches the theoretically obtained N_2 accessible surface area of FAU-Y (S_{BET} = 975 m^2/g, V_{mic} = 0.355 mL/g). A similar case was observed for MFI (S_{BET} = 393 m^2/g, V_{mic} = 0.157 mL/g). However, in this case, the underestimation of the surface area of the channels was compensated by the overestimation of the surface area of the intersections. For *BEA, S_{BET} represents the surface of the main channels (S_{BET} = 629 m^2/g, V_{mic} = 0.257 mL/g) without the surface of the small connecting channels. For MOR, S_{BET} represents the surface of the channels plus the surface of the side pockets (S_{BET} = 530 m^2/g, V_{mic} = 0.220 mL/g). Therefore for hierarchical micro-/mesoporous zeolites based on these structures, S_{BET} can be taken as the total surface area for further calculations. Another method based on the pre-adsorption of *n*-nonane in zeolites presenting 10-member ring (MR) channels was proposed for the characterization of pore volumes and surface areas of hierarchical MFI-type zeolites (such as nanocrystals, nanoboxes, and desilicated ZSM-5) [44]. It was observed that *n*-nonane filled the micropores of the MFI zeolite. Following the outgassing of the excess of *n*-nonane, the nitrogen isotherm of the pre-adsorbed sample was recorded, and the analysis of the isotherm revealed the presence of the fingerprint of the accessible mesoporous network. This was confirmed experimentally using a mechanical mixture of ZSM-5 and MCM-41 [44].

Herein, we present the corrected *t*-plot analysis and *n*-nonane pre-adsorption methods for the characterization of the micro-and mesopore volumes and surface areas of various hierarchical MFI-type zeolites. The results obtained using these methods were compared with the results obtained using the NLDFT methods (under conditions of Ar sorption at 87 K and N_2 sorption at 77 K) using the Micromeritics software.

2. Materials and Methods

2.1 Materials Synthesis

2.1.1 Micelle-templated ZSM-5: Synthesis

Micelle-templated ZSM-5 was prepared from commercial ZSM-5 treated with a solution of NaOH and octadecyltrimethyl ammonium bromide (C18TAB, from Aldrich). The commercial ZSM-5 was purchased from Zeolyst (ZSM-5 CBV 3024E; Si/Al = 15, NH_4^+ form; 10-MR; 3D; micropore size: interconnected channels; sinusoidal channels: 5.1 × 5.5 Å; straight channels: 5.3 × 5.6 Å; cavities in intersections: 8-10 Å). We followed the protocol reported by Goto et al. (2002) [7] for micro-/mesoporous ZSM-5 synthesis with slight modifications. We used a smaller amount of the surfactant and simplified the reported protocol. First, water, NaOH, and C18TAB were mixed at 323 K to obtain a clear solution. Following this, zeolite powder (2.5 g) was added to the mixture, and the mixture was stirred for 20 min. The molar composition of the mixture was calculated by assuming zeolites as pure silica (60 g/mol; 1 SiO_2: 0.1 C18TAB: n NaOH: 56 H_2O; n = 0.55). The mixture was then put in an autoclave at 388 K for 24 h. Following this, the pH was adjusted to 8.5 with HCl (2 M). A post-treatment step was conducted at 388 K for 24 h. Subsequently, the samples

were filtered and washed with water to arrive at neutral pH. The samples were dried at 373 K for 24 h and calcined in air at 823 K for 8 h.

2.1.2 ZSM-5 Nanosheet Spheres: Synthesis

The di-quaternary ammonium-type surfactant used for the synthesis of MFI-type nanosheet spheres or powder, ($[C_{22}H_{45}\text{-}N^{+}(CH_3)_2\text{-}C_6H_{12}\text{-}N^{+}(CH_3)_2\text{-}C_6H_{13}]Br_2$; $C_{22\text{-}6\text{-}6}$) was obtained in two steps following the procedure reported by Choi et al. [15].

The ZSM-5 nanosheet spheres were prepared using silica spheres of 50 µm diameter. The 50 µm amorphous porous silica spheres (Silica*Sphere*™) were obtained from *Silicycle*®. ZSM-5 spheres composed of nanosheets were hydrothermally synthesized (gel composition: 1 SiO_2: 0.3 Na_2O: 0.01 Al_2O_3: 0.18 H_2SO_4: 0.1 $C_{22\text{-}6\text{-}6}$: 40 H_2O [45]). The obtained gel was placed in a Teflon®-lined autoclave in a tumbling oven (30 rpm) at 423 K for 5 d. Subsequently, it was placed in an oven at 393 K and allowed to stand for 3 d. The organic surfactant was removed following the process of calcination. It was calcined in a furnace at 823 K for 6 h in an atmosphere of flowing air.

2.1.3 ZSM-5 Nanosheet Powder: Synthesis

ZSM-5 nanosheets were synthesized following the procedure described by Choi et al. [15] using tetraethoxy orthosilicate (Sigma-Aldrich) as silica source. A gel of molar composition 100 SiO_2: 30 Na_2O: 1 Al_2O_3: 10 $C_{22\text{-}6\text{-}6}$: 18 H_2SO_4: 4000 H_2O was prepared and heated in a Teflon®-lined autoclave in a tumbling oven (30 rpm) for 5 d at 423 K. The organic surfactant was removed following the process of calcination in a furnace at 823 K. The sample was calcined over a period of 6 h under conditions of airflow.

2.1.4 Silicalite-1 Nanosheet Spheres: Synthesis

Silicalite-1 nanosheet spheres were prepared using a silica source made of spherical particles of 20 µm diameter. The 20 µm amorphous porous silica spheres (Silica*Sphere*™) were obtained from *Silicycle*® [46]. The molar composition of the gel was 1 SiO_2: 0.3 Na_2O: 0.18 H_2SO_4: 0.1 $C_{22\text{-}6\text{-}6}$: 40 H_2O. The gel was heated at 383 K in static condition for 5 d. The organic surfactant was removed by calcination in a furnace at 823 K for 8 h under conditions of airflow.

2.1.5 ZSM-5 Desilication: Synthesis

The desilication of ZSM-5 (Si/Al = 40) was performed according to a protocol reported previously [44]. NaOH (30 mL, 0.2 M) and TBAOH (2 mL, 40% in water) were mixed in a propylene reactor. The mixture was heated to 343 K using an oil bath. ZSM-5 (1 g) was added to the mixture, and the mixture was stirred for 1 h at 343 K. The reaction was quenched in an ice bath. The reaction mixture was filtered. The precipitate was washed with 100 mL of distilled water, dried at 353 K for 12 h, and calcined in air at 823 K for 12 h.

2.1.6 Silicalite-1 Nanocrystals: Synthesis

Silicalite-1 nanocrystals were prepared using tetraethoxy orthosilicate (Sigma-Aldrich) as silica source under static conditions at 443 K over a period of 3 d. A clear solution of molar composition

1 SiO_2: 0.4 TPAOH: 35 H_2O, as described previously in [14], was used for synthesis. The organic surfactant was removed by calcination in a furnace at 823 K. The sample was calcined for 6 h under conditions of airflow.

2.1.7 ZSM-5 Nanocrystals: Synthesis

ZSM-5 nanocrystals were prepared following the protocol previously reported by us [13] using silica gel with particles of 75-150 µm and pore size of 3 nm (Sigma-Aldrich) as silica source. A solution of the final molar composition 1 $C_9H_{21}O_3Al$: 50 SiO_2: 450 H_2O: 10 TPAOH: 4 NaBr was used for synthesis. This mixture was heated in an oven at 443 K for 7 h in a stainless-steel Teflon®-lined autoclave. The organic surfactant was removed by calcining the sample in a furnace at 823 K over 6 h under conditions of airflow.

2.1.8 Al-MCM-41: Synthesis

Al-MCM-41(C18) (Si/Al = 15) was synthesized by mixing water, NaOH (Carlo Erba), $NaAlO_2$ (Carlo Erba), and octadecyltrimethylammonium bromide (C18TAB, from Aldrich) at 323 K to obtain a clear solution. Following this, silica powder (2.5 g) (Aerosil 200, Degussa) was added to the mixture, and the mixture was stirred for 20 min. The molar composition of the mixture was:1 SiO_2: 0.1 C18TAB: 0.066 $NaAlO_2$: 0.25 NaOH: 56 H_2O. The mixture was then transferred to an autoclave and placed in an oven at 388 K for 24 h. The recovered solid was filtrated, water-washed until neutral pH was reached, dried at 373 K for 24 h, and calcined under air at 823 K over a period of 8 h.

2.2 Characterization Techniques

2.2.1 N_2 Sorption at 77 K and Ar Sorption at 87 K

Different masses of materials were used to perform the gas sorption experiments. The mass was precisely determined: 20 mg of nanosheet ZSM-5 spheres, 50 mg of nanosheet silicalite-1 spheres, 80 mg of micelle-templated ZSM-5 (NaOH/Si = 0.55), 150 mg each of ZSM-5 and Silicalite-1 nanocrystals, and 180 mg each of desilicated ZSM-5 and nanosheet ZSM-5 were used for the experiments. Ar and N_2 sorption isotherms were recorded on a Micromeritics ASAP 2420 equipment at 87 K (liquid Ar) and 77 K (liquid N_2), respectively. Prior to recording the isotherms, the samples were outgassed at 363 K for 1 h. Following this, the samples were outgassed at 573 K for 15 h under vacuum to remove all traces of physisorbed water and volatile organic compounds (VOCs). The samples were outgassed again on the analysis ports at 363 K for 30 min and 573 K for 2 h prior to analyzing the samples. The dead volumes were measured post analysis to avoid pollution by He. A micropore dose of 10 cm^3/g was used to analyze the microporous part using both the gases.

The specific surface area was determined using the BET method. The application domain of the BET equation $(p/p_0)/[V(1-p/p_0) = f(p/p_0)$ was determined based on the superior limit reflected by the maximum of the Rouquerol curve $V(1-p/p_0) = f(p/p_0)$. This allows the determination of the linear BET range in an unambiguous way [42, 43, 47-50]. The BET area (S_{BET}) calculated based on the cross-sectional area of the nitrogen molecule (16.2 $Å^2$) for MFI is in agreement with the

nitrogen accessible surface area obtained by simulating the crystal framework [49]. S_{BET} represents the total surface area of the hierarchical MFI.

Mesopore diameters were calculated following the Broekhoff and De Boer (BdB) desorption method [51] at the inflection point of the desorption step, as it was demonstrated to be one of the most appropriate methods for the analysis of mesoporous materials such as MCM-41 [52]. The results obtained using the BdB method are in quite good agreement with the results obtained using the NLDFT method [43, 53].

The cumulative pore volumes, pore size distribution, and cumulative surface areas were calculated by the NLDFT method by analyzing the adsorption branch of the isotherms included in the Micromeritics software ("Microactive") and choosing the parameters corresponding to the cylindrical pores for micro-and mesopores and oxide surfaces at 87 K for Ar and 77 K for N_2.

2.2.2 Pre-adsorption of *n*-Nonane

Approximately 40 mg each of the hierarchical MFI-type zeolites were placed in a SETARAM microbalance, and the sample was outgassed under conditions of secondary vacuum at 573 K over a period of 10 h. After cooling the sample to room temperature, the materials were exposed to vapors of *n*-nonane over a period of 2 h. Following this, the samples were subjected to secondary vacuum conditions at room temperature until mass stabilization was achieved. The mass of *n*-nonane was precisely determined and expressed as x g of *n*-nonane for 1 g of the zeolite filled with *n*-nonane, hence 1-x g of zeolite. The N_2 sorption isotherms were recorded at 77 K using a Micromeritics 3FLEX instrument. The volume and surface areas of the zeolites containing *n*-nonane were expressed per g of the zeolite filled with *n*-nonane. The values had to be corrected to obtain the values (volume and surface area) per g of the zeolites and be compared to the values obtained with the starting zeolite (before *n*-nonane adsorption). This was achieved by divided the volumes and the surface areas expressed per mass of zeolites filled with n-nonane by (1-x).

3. Results and Discussion

3.1 Analysis of t-plots

The presence of micropores in a material can be validated by plotting the amount of nitrogen adsorbed (on the porous solid under study) as a function of the amount of nitrogen adsorbed on a non-porous (or macroporous) reference solid with similar surface properties as the material under study. For zeolites, non-porous silica was used for recording the reference isotherm [41-43]. The statistical film thickness (*t*) is defined as the amount of adsorbed nitrogen (V_a) divided by the amount of nitrogen adsorbed by the monolayer (V_m; calculated using the BET equation) of the non-porous reference solid multiplied by the size of a nitrogen molecule:

$$t(\text{Å}) = 3.54(V_a/V_m) \quad (1)$$

For the studied porous material, after recording the nitrogen isotherm, the relative pressure (p/p_0) can be converted into film thickness (*t*) as follows:

For $0.009 < p/p_0 < 0.12$

$$\mathrm{t1} = 1.62973 + 76.4748(p/p_0) - 2171.7914(p/p_0)^2 + 41734.77357(p/p_0)^3 \\ -465290.41181(p/p_0)^4 + 2.72432\ 10^6(p/p_0)^5 - 6.43708\ 10^6(p/p_0)^6 \quad (2)$$

For $0.13 < p/p_0 < 0.60$:

$$\mathrm{t2} = 3.07721 + 5.64019(p/p_0) \quad (3)$$

For $0.60 < p/p_0 < 0.75$:

$$\mathrm{t3} = 4592.05803 - 38117.31548(p/p_0) + 131602.19741(p/p_0)^2 - 241680.40239(p/p_0)^3 \\ +249079.8569(p/p_0)^4 - 136632.44762(p/p_0)^5 + 31182.4149(p/p_0)^6 \quad (4)$$

For $0.75 < p/p_0 < 0.90$:

$$\mathrm{t4} = 2098.4 - 10711(p/p_0) + 18954(p/p_0)^2 - 9197.5(p/p_0)^3 \\ -10624(p/p_0)^4 + 14046(p/p_0)^5 - 4553(p/p_0)^6 \quad (5)$$

with *t* expressed in Å.

If adsorption on both solids (porous and reference solids) proceeds via the same mechanism, i.e., via multilayer adsorption, the comparative plot (*t*-plot) is linear in the whole pressure range. This is true for macroporous solids. Under these conditions, the surface area can directly be calculated from the slope of the *t*-plot as follows:

$$\mathrm{S}(\mathrm{m}^2/\mathrm{g}) = (\mathrm{slope}/646) \times 10^4 t(\text{Å}) \quad (6)$$

The ratio of liquid nitrogen density ($\rho_{N2\text{-}liq}$) to nitrogen gas (STP) density ($\rho_{N2\text{-}gas}$) is given as follows:

$$\rho_{N2-liq}/\rho_{N2-gas} = 646 \quad (7)$$

When the solid under study contains mesopores, adsorption initially proceeds via the formation of multilayers (the case is identical to the case observed for macroporous or non-porous reference systems). Capillary condensation takes place at high relative pressure conditions (generally $p/p_0 > 0.3$). Consequently, the initial part of the *t*-plot appears linear. The plot exhibits an upward deviation from linearity in the capillary condensation region and achieves a plateau when the mesopores are filled with the condensed adsorbate (Figure 1). This type of *t*-plot can be used to evaluate the mesopore volume and specific surface area attributable to the mesopore plus external surface $(S_{mes+ext})_{tpt}$ in the linear plot in the low-pressure region and the external surface area (S_{ext}) in the high-pressure range post-capillary condensation (Figure 1). The total pore volume (V_{tot}) or mesopore volume is obtained for the first fitting point of the second linear fit of the *t*-plot at high relative pressure conditions. $(S_{mes+ext})_{tpt}$ is obtained from the slope of the first linear plot. This value is comparable to the total surface area calculated using the BET equation (S_{BET}). This type of a *t*-plot also provides evidence of the absence of microporosity, as the initial linear part of the *t*-plot passes through the origin (Figure 1). The characteristics of the purely

mesoporous material Al-MCM-41(C18) (Si/Al = 15) have been presented (Figure 1): V_{mic} = 0, V_{mes} = 0.707 mL/g, S_{BET} = 846 m^2/g, $S_{mes+ext}$ = 851 m^2/g, S_{ext} = 226 m^2/g, S_{mic} = 0, S_{mes} = 625 m^2/g.

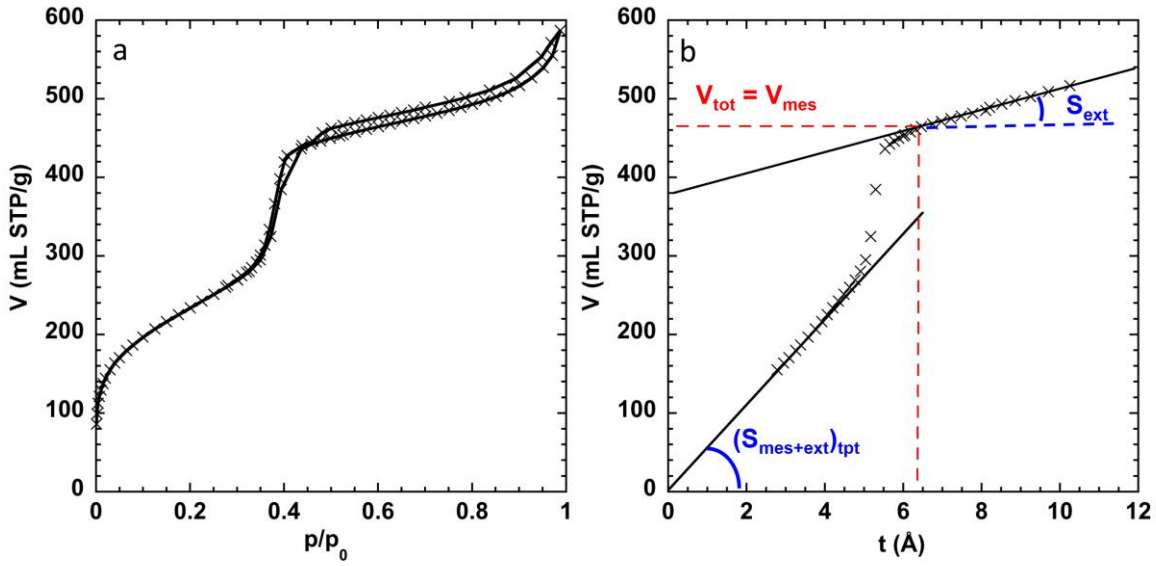

Figure 1 (a) N_2 sorption isotherm recorded at 77 K for Al-MCM-41(C18) and (b) corresponding *t*-plot.

When the solid under study is characterized by the presence of micropores, the presence of the latter manifests itself under conditions of enhanced low-pressure adsorption. Consequently, the initial part of the *t*-plot (that is, the region of low pressures or the region of low *t* values) exhibits a sharp increase in pore volume. The plot levels off at higher pressure regions where the micropores are filled with a condensed adsorbate. The real micropore volume $(V_{mic})_{real}$ is given by the total volume (V_{tot}) in Figure 2. However, for materials containing micropores and mesopores (Figure 3), the linear extrapolation of the first slope with an intercept on the Y-axis in the plot of *V* versus *t* is generally assessed to determine the micropore volume $(V_{mic})_{tpt}$. For microporous solids such as ZSM-5, $(V_{mic})_{tpt} < (V_{mic})_{real}$ (Figure 2). Therefore, the extrapolation of the first slope of the *t*-plot leads to an underestimation of micropore volume in hierarchical MFI structured zeolites [43]. Likewise, the mesoporous plus external surface area $(S_{mes+ext})_{tpt}$ determined from the *t*-plot of ZSM-5 is overestimated as it should be equal to the external surface area. Only the external surface area (S_{ext}) should be considered in purely microporous samples. As for ZSM-5, in hierarchical MFI materials, the first slope of the *t*-plot (Figure 3) results in an overestimation of the mesopore plus external surface area $(S_{mes+ext})_{tpt}$. The properties of ZSM-5 (Si/Al = 15) (Figure 2) have been presented: V_{mic} = 0.162 mL/g, V_{mes} = 0, S_{BET} = 372 m^2/g, S_{ext} = 53 m^2/g, S_{mic} = 319 m^2/g, S_{mes} = 0.

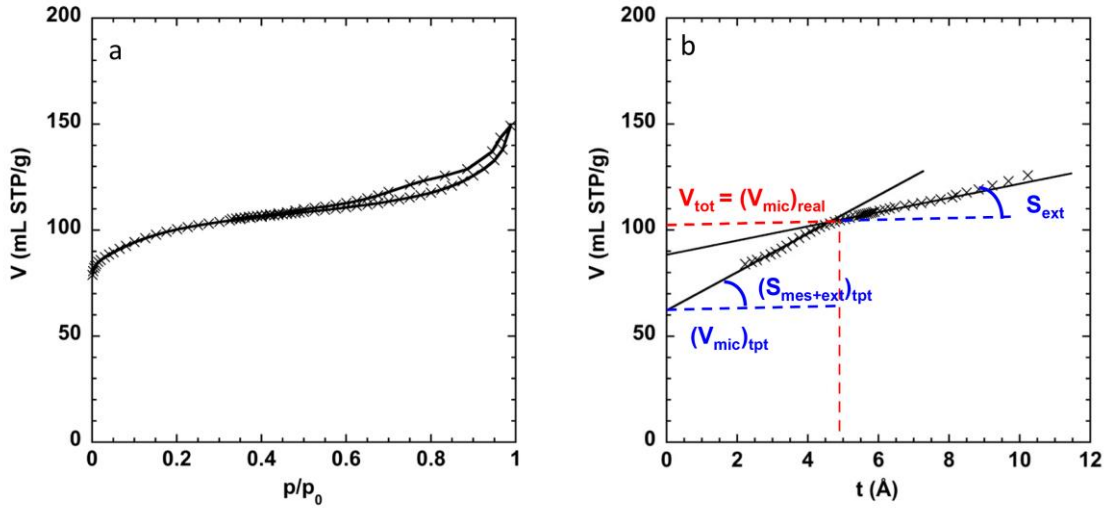

Figure 2 (a) N_2 sorption isotherm at 77 K of ZSM-5 (Si/Al = 15) and (b) corresponding *t*-plot.

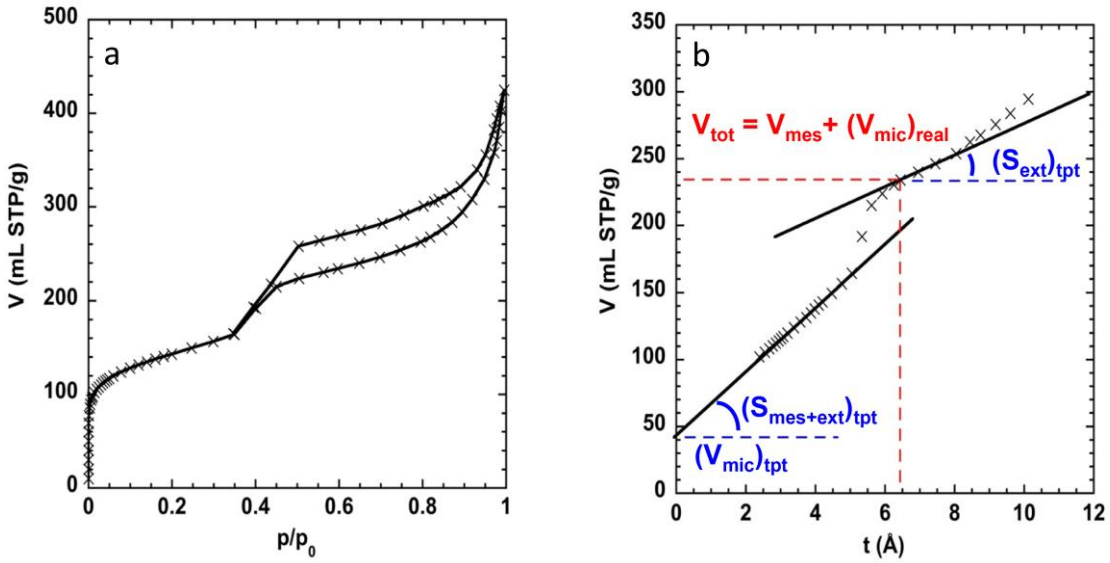

Figure 3 (a) N_2 sorption isotherm recorded at 77 K for hierarchical ZSM-5 (Si/Al = 15) prepared following the micelle-templating (NaOH/Si = 0.55) method and (b) corresponding *t*-plot.

When the solid under study is characterized by the presence of both micropores and mesopores, the shape of the *t*-plot becomes more complex, and it reflects the deviation from linearity. The deviation from linearity can be attributed to the process of micropore filling and capillary condensation (Figure 3). The total pore volume (V_{tot}) (of mesopores and micropores) is obtained for the first fitting point of the second linear fit of the *t*-plot at high relative pressure conditions (Figure 3).

Theoretically, the intercept of the first linear fit can be analyzed to assess the micropore volume $(V_{mic})_{tpt}$ and the slope of the mesopore plus external surface area $(S_{mes+ext})_{tpt}$ (Figure 3). As for pure ZSM-5 (Figure 2), this extrapolation results in the underestimation of the real micropore volume and an overestimation of the surface area. Mechanical mixtures of ZSM-5 and Al-MCM-

41(C18), characterized by defined micropore and mesopore volumes and surface areas, were prepared to determine the corrections needed to calculate the real micropore volume (V_{mic*}) and the real mesopore plus external surface area ($S_{mes+ext*}$) from the *t*-plots [43]:

$$for\ all\ (V_{mic}/V_{tot})_{tpt} \quad S_{mes+ext^*} = (S_{mes+ext})_{tpt}\left[1 - (V_{mic}/V_{tot})_{tpt}\right] \tag{8}$$

$$for\ 0.04 < (V_{mic}/V_{tot})_{tpt} < 0.1 \quad V_{mic^*} = 2(V_{mic})_{tpt} \tag{9}$$

$$for\ (V_{mic}/V_{tot})_{tpt} > 0.15 \quad V_{mic^*} = 1.6(V_{mic})_{tpt} \tag{10}$$

The external surface area $(S_{ext})_{tpt}$ is usually determined from the slope of the second linear fit of the *t*-plot (Figure 3).

However, for hierarchical ZSM-5 systems prepared following the micelle-templating method and characterized by a mesopore diameter of approximately 4 nm (capillary condensation occurs at approximately p/p_0 = 0.4) (Figure 3), the existence of secondary large mesoporosity results in the overestimation of $(S_{ext})_{tpt}$. The secondary mesoporosity, in which pore filling occurs immediately after capillary condensation, is evidenced by the horizontal hysteresis in the nitrogen adsorption isotherm, resulting in cavitation. Hence, only (V_{tot}), $(S_{mes+ext})_{tpt}$, and $(V_{mic})_{tpt}$ are extracted from *t*-the plots for hierarchical MFI (Figure 3), and corrections are applied (Eq. 8-10) to obtain ($S_{mes+ext*}$) and (V_{mic*}). Following this, the micropore surface area (S_{mic}) and the mesopore volume (V_{mes}) were calculated as follows:

$$S_{mic} = S_{BET} - (S_{mes+ext^*}) \tag{11}$$

$$V_{mes} = V_{tot} - (V_{mic^*}) \tag{12}$$

3.2 Pre-adsorption of n-Nonane: Method

Another method to calculate the pore volumes and surface areas of hierarchical MFI involves the pre-adsorption of *n*-nonane followed by the recording of the N_2 adsorption isotherm at 77 K. The method followed for realizing the pre-adsorption of *n*-nonane was introduced by Gregg and Langford in 1969 [54]. The method was used to determine the micropore volume and the external surface area of microporous carbons. This method was then validated by Rouquerol et al. in 1993 [55] for zeolites with MFI-structure (such as large micronic crystals of silicalite-1). The technique is based on the fact that *n*-nonane, with a minimum kinetic diameter of 0.43 nm, desorbs infinitely slowly from narrow ultramicropores (< 0.6 nm) at ambient temperature conditions. *n*-Nonane has strong physisorption energy in such micropores, which consequently results in a high energy barrier for its desorption. The nitrogen isotherm at 77 K, obtained following the pre-adsorption of *n*-nonane, indicated the presence of weak adsorbate-adsorbent interactions and reflected the total inaccessibility of nitrogen into the microporous structure. This allowed the calculation of the external surface area of large micronic crystals of silicalite-1 (< 0.2 m^2/g). *n*-Nonane molecules are very strongly trapped in such ultramicropores. This is not the case for wider micropores of zeolites such as AlPO4-5 (0.74 nm), MOR (0.70 × 0.65 nm), or FAU (windows: 0.74 nm), where *n*-nonane is partially desorbed under conditions of vacuum. Depending on the pore structure, the retention of *n*-nonane molecules in ultramicropores may also result in the blocking of some wider pores, and the method allows the determination of the volume of the wider pores (as mesopores) that are in

direct contact with the exterior of the crystal. The difference in the volumes obtained by analyzing the nitrogen isotherms recorded before and after the pre-adsorption of *n*-nonane reflects the micropore volume (or micropore volume plus the volume of the embedded pores not connected to the exterior). The pre-adsorption of *n*-nonane results in the blocking of the entire micropore volume of the MFI structured zeolites (commensurate freezing). Hence, the successive N_2 physisorption process helps in achieving the isotherm where the micropore volume has no influence. The isotherm then reflects the mesopore connected to the exterior of the hierarchical ZSM-5.

This method for hierarchical MFI type zeolites has been validated previously by some of us using the mechanical mixture of MFI and MCM-41 [44]. The N_2 adsorption isotherm of MFI pre-adsorbed with *n*-nonane solely reflects the adsorption on the external surface of ZSM-5 (Figure 4). The N_2 adsorption isotherm of MCM-41 pre-adsorbed with *n*-nonane is similar to the isotherm recorded before n-nonane adsorption (Figure 4). For mechanical mixtures of MFI and MCM-41, the micropore volume (V_{mic}) can be directly calculated from the volume difference obtained from the two N_2 isotherms (recorded before (V_{N2}) and after *n*-nonane pre-adsorption (V_{C9}) at a given p/p_0 pressure) (Figure 5). The relative pressure (p/p_0) at which the volume difference is to be calculated should be higher than 0.4. Under these conditions, all nitrogen molecules are ordered inside the micropores of MFI. The mesopore volume is defined as the total pore volume obtained from the N_2 isotherms recorded after *n*-nonane pre-adsorption. The value is determined at the end of the mesopore filling process ($V_{tot\text{-}C9}$). The micropore surface area is the difference between the BET surface areas calculated from the N_2 isotherms recorded before ($S_{BET\text{-}N2}$) and after *n*-nonane pre-adsorption ($S_{BET\text{-}C9}$). The mesopore plus external surface area ($S_{mes+ext}$) is the BET surface area calculated from the N_2 isotherms recorded after *n*-nonane pre-adsorption ($S_{BET\text{-}C9}$). It should be remembered that *n*-nonane mass corrections should be performed before conducting the calculations to obtain the surface areas and pore volumes expressed per g of the zeolite (and not per g of the zeolite filled with *n*-nonane).

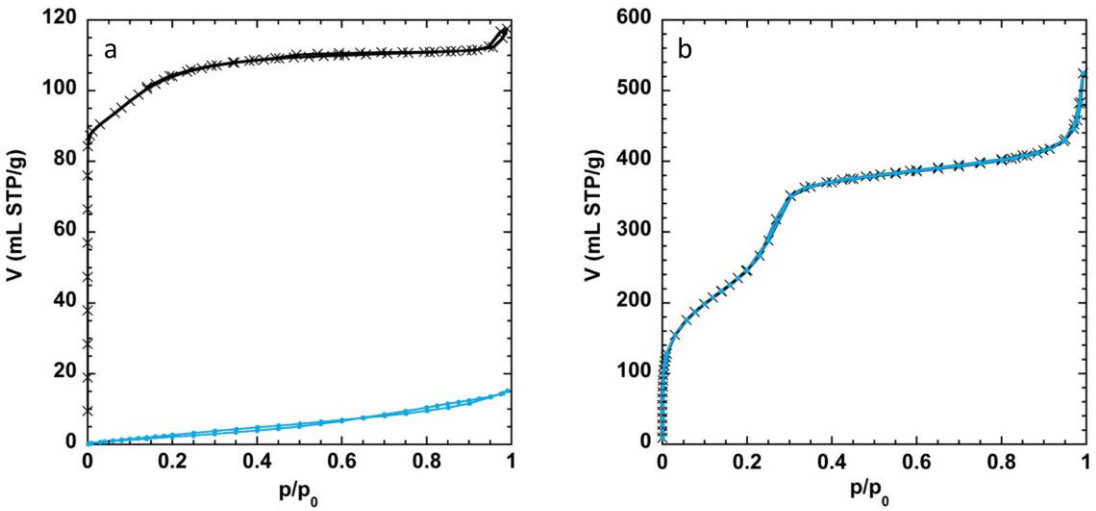

Figure 4 N_2 sorption isotherms recorded at 77 K for (a) ZSM-5 (Si/Al = 40) and (b) Si-MCM-41(C16) in the presence (blue points) and absence (black crosses) of pre-adsorbed n-nonane.

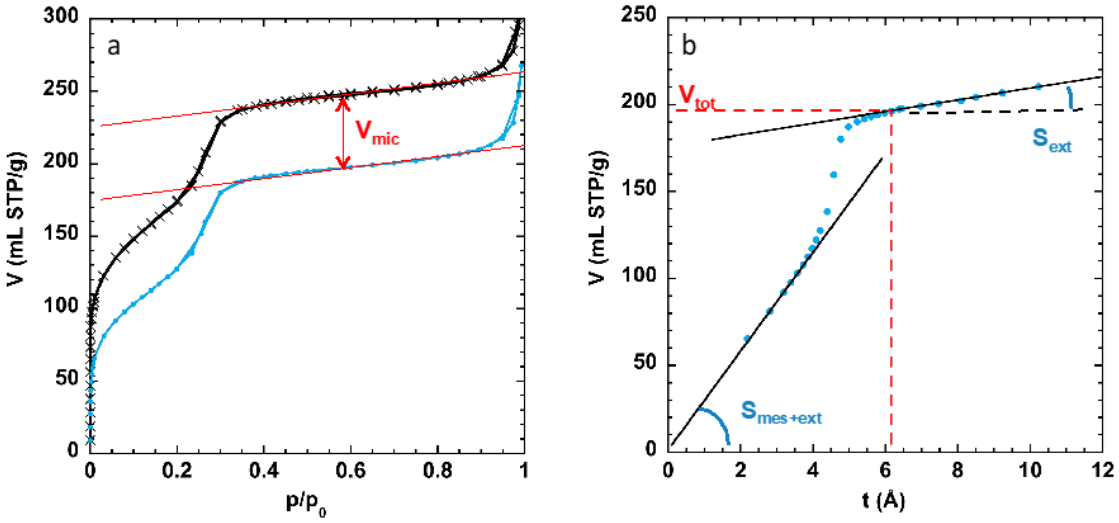

Figure 5 (left) N_2 sorption isotherms recorded at 77 K for the mechanical mixture prepared with 50 wt.% of ZSM-5 (Si/Al = 40) and 50 wt.% of Si-MCM-41(C16) in the presence (blue points) and absence (crosses) of pre-adsorbed *n*-nonane. (right) The Corresponding *t*-plot obtained following the pre-adsorption of *n*-nonane showing the absence of microporosity.

The *t*-plots were analyzed based on the N_2 isotherms recorded post *n*-nonane pre-adsorption on the mechanical mixture of MFI and MCM-41. A linear fit in the low-pressure range (low *t*), passing through the origin and demonstrating the absence of microporosity, was obtained (Figure 5). The *n*-nonane molecules completely fill the micropores and do not get evaporated during the outgassing step. The resulting mesopore surface area plus external surface area ($S_{mes+ext-C9}$) is comparable to the BET surface area (S_{BET-C9}). The method of *n*-nonane pre-adsorption allows the calculation of the mesopore volume, micropore volume, micropore surface area, and mesopore plus external surface area.

In summary, the following equations can be used to characterize the micropore and mesopore volumes and the surface areas of the hierarchical MFI-type zeolites using the *n*-nonane pre-adsorption method:

$$V_{mic} = V_{N2} - V_{C9} \quad (at \;\; p/p_0 > 0.4) \tag{13}$$

$$V_{mes} = V_{tot-C9} \tag{14}$$

$$S_{mic} = S_{BET-N2} - S_{BET-C9} \tag{15}$$

$$S_{mes+ext} = S_{BET-C9} \tag{16}$$

with X_{C9} meaning the volume (X = V) or surface area (X = S) calculated from the nitrogen isotherms of the zeolite after preadsorption of *n*-nonane (and mass correction).

For the mechanical mixtures of MFI and MCM-41, the mesopore volume (V_{mes-C9}) and surface areas ($S_{mes+ext-C9}$) determined following the *n*-nonane pre-adsorption method are in good agreement with the predicted calculated values (calculated from the weight percentages ($V_{mes-cal}$

and $S_{mes+ext-cal}$)) (Figure 6). The micropore surface areas (S_{mic-C9}) and volumes (V_{mic-C9}) are in good agreement with the predicted calculated ($S_{mic-cal}$) and ($V_{mic-cal}$) values, respectively (Figure 7).

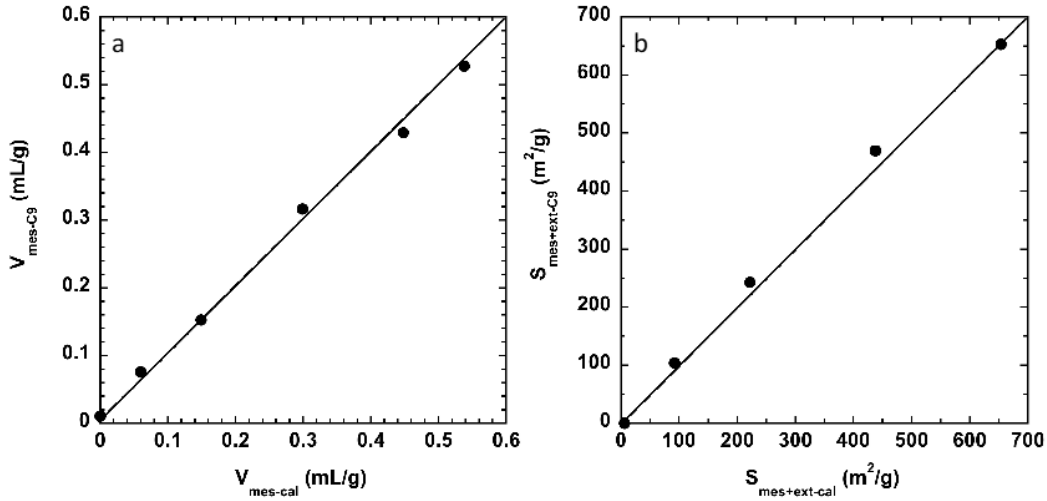

Figure 6 (a) Mesopore volumes and (b) mesopore surface areas recorded post *n*-nonane pre-adsorption for the mechanical mixture of ZSM-5 (Si/Al = 40) and Si-MCM-41(C16). The values are compared with the predicted calculated values for each material.

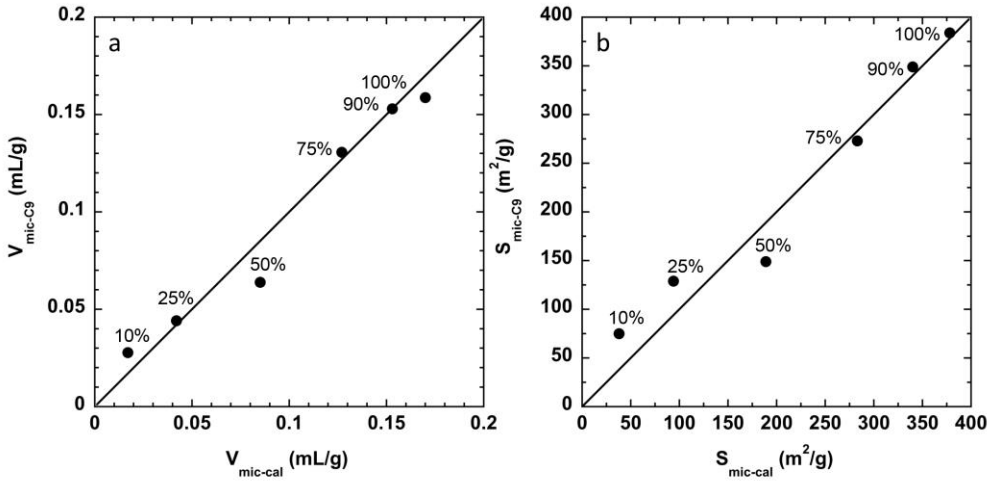

Figure 7 (left) Micropore volumes (taken at $p/p_0 = 0.42$) and (right) micropore surface areas determined from the nitrogen isotherms recorded for the mechanical mixtures of ZSM-5 (Si/Al = 40) and Si-MCM-41(C16) pre-adsorbed with *n*-nonane. The values were compared with the predicted calculated values determined based on the weight percentage of each material.

3.3 Characterization of the Hierarchical MFI-type Zeolites

Various hierarchical MFI-based zeolites (ZSM-5 or Silicalite-1) were prepared following different methods (Figure 8):

1. Micelle-templated Na-ZSM-5 was prepared based on a modification of the protocol described by Goto et al. [7]. The molar ratio was NaOH/Si = 0.55 and C18TAB/Si = 0.1. A commercial ZSM-5 (Si/Al = 15) was used for sample preparation [43].
2. Na,H-ZSM-5 (Si/Al = 41) spheres (50 µm in diameter) composed of 2 nm-thick nanosheets were prepared following the pseudomorphic synthesis method outlined by Moukahhal et al. [45].
3. H,Na-ZSM-5 (Si/Al = 45) powder composed of 2 nm-thick nanosheets was obtained following the protocol outlined by Choi et al. [15].
4. Silicalite-1 Spheres (diameter: 20 µm) composed of 3 nm-thick nanosheets were prepared following the pseudomorphic synthesis method reported by Moukahhal et al. [46].
5. Desilicated ZSM-5 (Si/Al = 40) was synthesized following the protocol outlined by Batonneau-Gener et al. [44].
6. Silicalite-1 nanocrystals with an average diameter of 200 nm were synthesized following the method reported by Huve et al. [14].
7. ZSM-5 (Si/Al = 21) nanocrystal aggregates of primary particles (diameter: 50-150 nm) exhibiting cuboid morphology and characterized by smooth edges were synthesized following the method reported by El Hanache et al. [13].

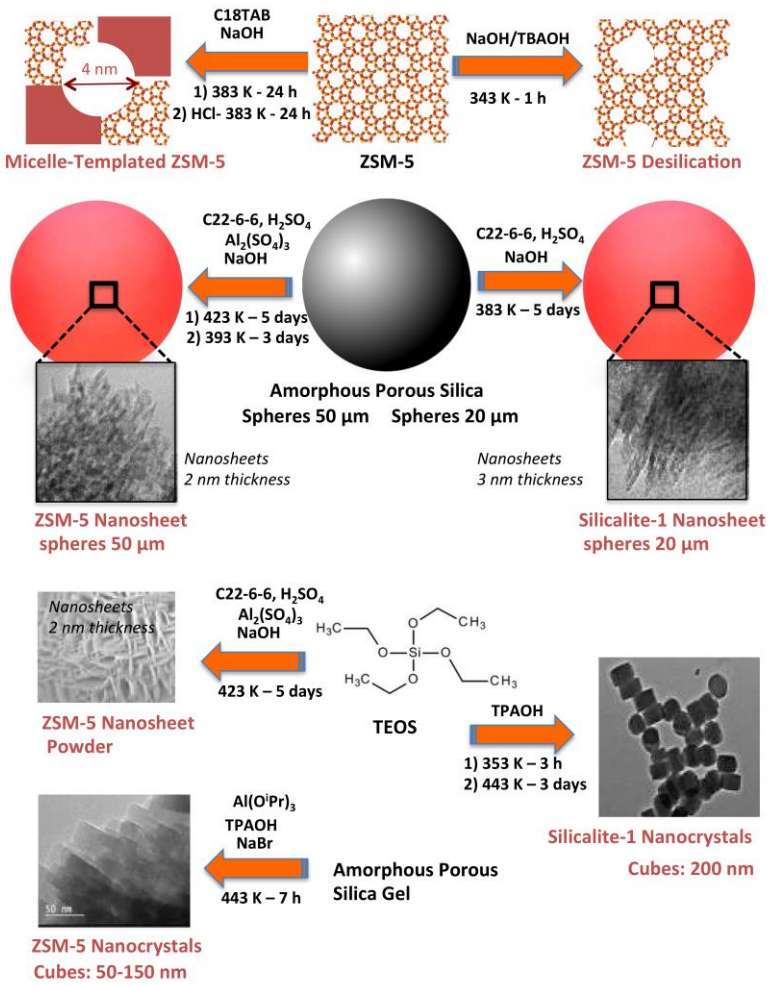

Figure 8 Schematic representation of the method of synthesis of different hierarchical MFI-type zeolites.

The nitrogen adsorption isotherms at 77 K for the hierarchical MFI were recorded (Figure 9), and the micro-and mesopore volumes and the micropore and mesopore plus external surface areas were evaluated following the *n*-nonane pre-adsorption method and by analyzing the *t*-plots (Figure 3, Figure 10, and Figure S1). The determination by *t*-plot method was followed by specific corrections for the ZSM-5 hierarchical zeolites (Eq. 8-10).

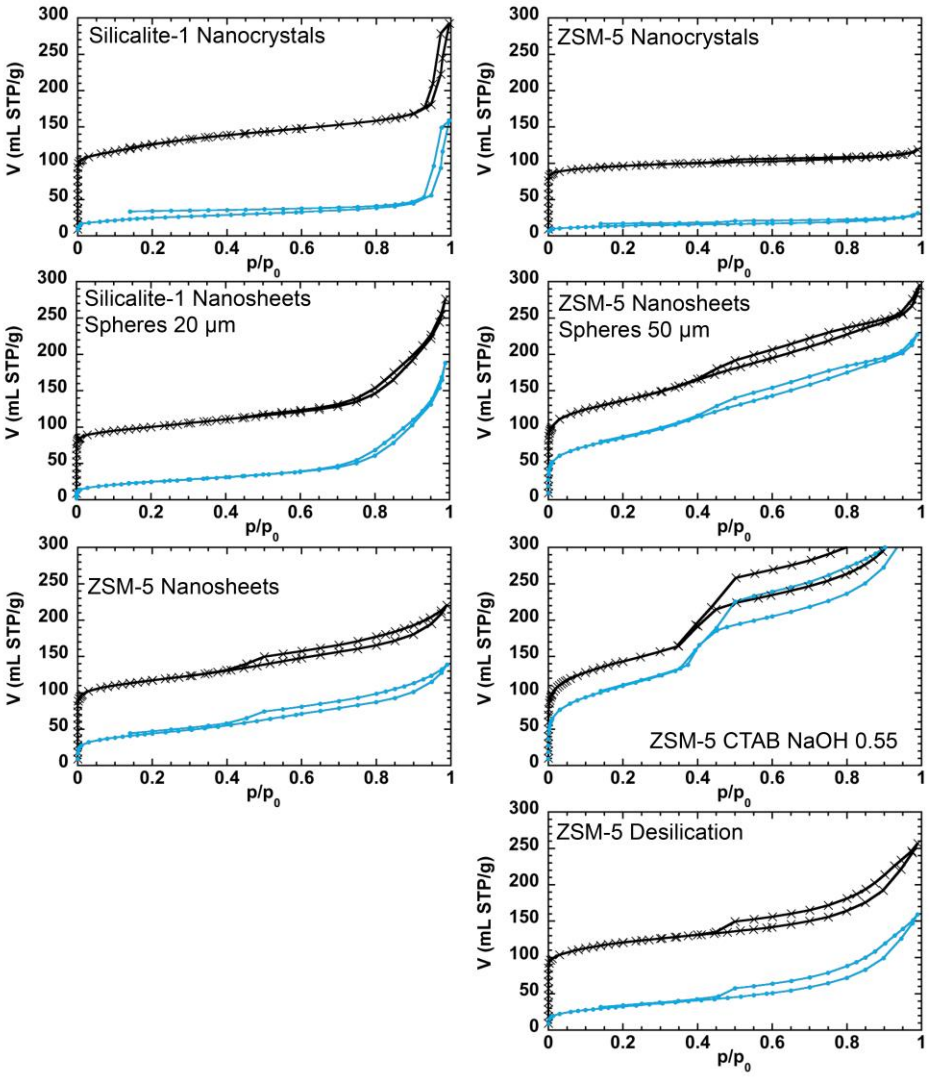

Figure 9 N_2 sorption isotherms recorded at 77 K for different hierarchical MFI-type zeolites. The isotherms were recorded (crosses) before and (circles) after *n*-nonane adsorption and outgassing processes.

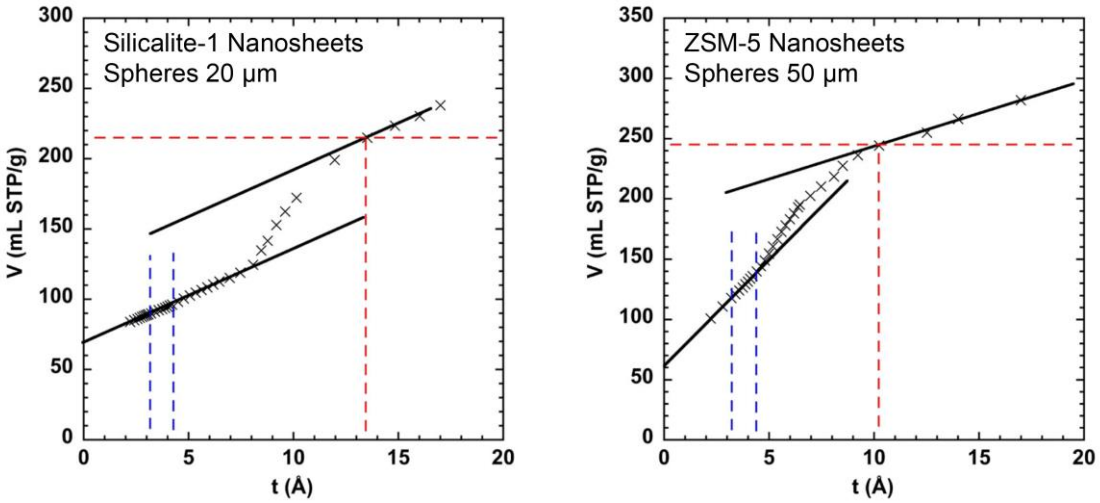

Figure 10 Analysis of *t*-plots generated for hierarchical ZSM-5 systems. Range of *t* for the first fit at low *t* (dashed blue lines) and the starting point of *t* (vertical red dashed line) for the second fit at high *t* correspond to (horizontal red dashed line) the "total" pore volume (micropore + mesopore volumes).

For comparison, Ar adsorption isotherms were recorded at 87 K, and the non-local-density functional theory (NLDFT) method was used to calculate the micropore and mesopore volumes from the adsorption branch of the isotherms (N_2 at 77 K and Ar at 87K). The cumulative pore volume curves as a function of pore diameter were generated using a model of cylindrical pores for oxide surfaces (Figure S2).

In the NLDFT approach, adsorption isotherms in model pores are calculated based on the intermolecular potentials of the fluid--fluid and solid--fluid interactions. The local density of the adsorbate confined in a pore at a given chemical potential and temperature is determined by minimization of the grand thermodynamic potential to describe the process of capillary condensation/desorption of the adsorbate into a pore [53]. The method allows the calculation of a particular adsorbate/adsorbent pair from a series of theoretical isotherms in pores of given shapes but varying widths. The analysis of the pore size distribution is based on the solution of the experimental adsorption isotherm compared with the series of theoretical isotherms. Intermolecular potentials for both fluid--fluid and solid--fluid interactions were considered. Hence, the NLDFT method could be used to obtain the thermodynamic and density profiles of the confined fluids. The adsorbed phase could be described at a molecular level. It captures the essential features of the pore-filling mechanism and the mechanism of mesopore capillary condensation, desorption, and hysteresis. The drawback of the conventional NLDFT method lies in the assumption of a smooth and homogeneous surface of the adsorbent. The energetic heterogeneity of the surface of the adsorbent is neglected, resulting in the generation of multiple steps in the adsorption isotherms. These are not observed in the experimental adsorption isotherms. These steps are associated with a layering transition associated with the formation of a monolayer, a second adsorbed layer, and so forth. This can cause prominent artifacts in the NLDFT pore size distributions at approximately 1 and 2 nm for carbons [56] and at approximately 3 and 4 nm for the MCM-41-type silica [31, 53]. The condensation/evaporation transition in mesopores is vertical. This is not observed in experimental isotherms. This can be attributed to pore size

heterogeneity and the non-uniformity in the pore channels. However, the calculated condensation and equilibrium transitions correspond to the inflection points of the experimental adsorption and desorption isotherms, respectively. Several approaches have been suggested to consider the roughness and heterogeneity of the pore wall surfaces of most adsorbents. Promising methods that can be used to avoid these artifacts are in their developing stages. These methods include the quenched solid density functional theory (QSDFT) method [31, 56].

Analysis of the nitrogen isotherms recorded at 77 K for the hierarchical MFI (Figure 9) revealed the presence of different types of materials with different characteristics (surface areas, pore volumes, and pore-size distributions) (Table 1, Tables S1-S7).

Table 1 Textural properties of the hierarchical MFI-type zeolites.

		Corrected t-plot		NLDFT N_2 2 nm		
	S_{BET} m^2/g	$S_{mes+ext*}$ m^2/g	S_{mic*} m^2/g	V_{mic} mL/g	[a]V_{tot} mL/g	V_{mes} mL/g
MFI structure (simulation [43])	393	0	393	0.157	0.157	0
ZSM-5 nanocrystals	382	33	349	0.142	0.167	0.025
Silicalite-1 nanocrystals	443	99	344	0.186	0.449	0.263
Silicalite-1 nanosheets Spheres	372	93	279	0.129	0.433	0.304
ZSM-5 nanosheets Spheres	491	208	283	0.112	0.464	0.352
ZSM-5 nanosheets Powder	440	98	342	0.152	0.340	0.188
Micelle-Templated ZSM-5	517	305	212	0.093	0.619	0.247[b] 0.279[c]
Desilicated ZSM-5	446	84	362	0.139	0.402	0.263
Al-MCM-41(C18)	846	851	0	0	0.707	0.707

[a]total pore volume at p/p_0 = 0.98. [b]mesopore volume of ordered pores (4 nm). [c]volume of mesopores larger than 4 nm.

ZSM-5 nanocrystals present a type I isotherm [32] which is characteristic of pure microporous materials. The nanocrystals (50-150 nm) are stuck on each other and cannot generate intercrystalline pores with diameters <50 nm. These conclusions were arrived by analyzing the nitrogen adsorption isotherm. The mercury porosimetry technique should be used to determine the intercrystalline pore size and volume. The total surface area was (S_{BET}) 382 m^2/g with an external surface area of 33 m^2/g (Table S7). The surface area was close to the simulated surface area of the MFI structure (S_{BET} = 393 m^2/g, V_{mic} = 0.157 mL/g) [43]. The cumulative pore volumes (NLDFT N_2) at 2 and 7 nm were V_{mic} = 0.142 mL/g and V_{tot} = 0.167 mL/g, respectively (Table 1, Table S7).

Silicalite-1 nanocrystals (200 nm) present an isotherm of type I with an additional narrow vertical hysteresis at high relative pressures (p/p_0 = 0.95), reflecting the intercrystalline pores of diameter > 35 nm and volume > 0.23 mL/g. The mercury porosimetry technique should be used to accurately determine the intercrystalline pore diameter and volume. The total surface area of silicalite-1 nanocrystals was (S_{BET}) 444 m^2/g, and the mesopore plus external surface area was 99 m^2/g. The cumulative pore volume (NLDFT N_2) was V_{mic} = 0.186 mL/g (Table 1, Table S6).

Silicalite-1 nanosheets spheres (20 µm) present an isotherm of type I with an additional narrow hysteresis extended on a large range of relative pressure $0.7 < p/p_0 < 1$. This kind of hysteresis has been observed in silica with inverted cone-shaped pores (maximum diameter: 30 nm; depth: 100 nm) [57]. The associated pore volume is greater than 0.29 mL/g. The mercury porosimetry technique should be used to accurately evaluate the pore diameter and volume. The total surface area was (S_{BET}) 372 m^2/g with a mesopore plus external surface area of 93 m^2/g. The cumulative pore volumes (NLDFT N_2) were V_{mic} = 0.129 mL/g (Table 1, Table S4).

ZSM-5 nanosheet spheres (50 µm) present an isotherm of type I. A linear increase in the extent of nitrogen adsorption was observed over a very broad range of relative pressure ($0.2 < p/p_0 < 0.9$). A narrow hysteresis region is observed. This kind of hysteresis has been observed in silica systems where the pore depth is inferior to the pore diameter [58]. The distribution of pore diameter is broad (2-22 nm), and the pore volume is 0.25 mL/g. Supplementary nitrogen uptake occurs in very high-pressure regions. Secondary larger pores (> 50 nm) exist, which should be analyzed using the mercury porosimetry technique. The total surface area was (S_{BET}) 491 m^2/g, and the mesopore plus external surface area was 208 m^2/g. The cumulative pore volume (NLDFT N_2) was V_{mic} = 0.112 mL/g (Table 1, Table S2).

ZSM-5 nanosheet powder presents an isotherm of type I. A linear increase in the extent of nitrogen adsorption was observed over a broad range of relative pressure ($0.2 < p/p_0 < 1$). A narrow horizontal hysteresis region of type H4 [32], characteristic of cavitation (attributable to the presence of large embedded pores (> 50 nm) connected to the exterior of the crystals via pores of diameter < 5 nm), was observed. These can be small mesopores or the micropores of the zeolites. This type of hysteresis can be observed in aggregates of plate-like particles. The total surface area was (S_{BET}) 440 m^2/g, and the mesopore plus external surface area was 98 m^2/g. The cumulative pore volume (NLDFT N_2) was V_{mic} = 0.152 mL/g (Table 1, Table S3).

Micelle-templated ZSM-5 presents an isotherm of type IV. It is typical of a mesoporous material, and a step in the adsorption profile is observed at p/p_0 0.4. It corresponds to ordered mesopores with a diameter of 4 nm (e.g., Al-MCM-41) (Figure 1). An additional horizontal hysteresis at higher relative pressure regions, characteristic of a cavitation phenomenon attributable to the existence of large embedded pores (> 50 nm) connected to the exterior of the crystal via ordered mesopores of diameter 4 nm, was also observed. The total surface area was (S_{BET}) 517 m^2/g, and the mesopore plus external surface area was 305 m^2/g. The cumulative pore volume (NLDFT N_2) was V_{mic} = 0.093 mL/g (Table 1, Table S1).

Desilicated ZSM-5 presents an isotherm similar to the one recorded for the ZSM-5 nanosheet powder. A type I isotherm, exhibiting a linear increase in the extent of nitrogen adsorption (over a very broad range of relative pressure ($0.2 < p/p_0 < 1$)) and featuring a narrow horizontal hysteresis of type H4 [32] that is characteristic of a cavitation phenomenon attributable to the existence of large embedded pores (> 20 nm; connected to the exterior via either small mesopores (diameter < 5 nm) or micropores of the zeolites) is observed. The total surface area was S_{BET} 446 m^2/g, and the mesopore plus external surface area of 84 m^2/g. The cumulative pore volumes (NLDFT N_2) gives V_{mic} = 0.152 mL/g (Table 1, Table S5).

The cumulative micropore volumes of hierarchical MFI-type zeolites (0.09 - 0.19 mL/g) calculated following the NLDFT method were taken at a pore width of 2 nm (Table 1). The end of the micropore filling and the rearrangement of the Ar and N_2 molecules were considered to be ended at this pore width (Figure S2, Tables S1-S7). Micropore volumes determined using the

NLDFT method using N_2 at 77 K were lower (-0.006 to -0.044 mL/g, depending on the hierarchical MFI-type zeolite) than the micropore volumes determined with Ar at 87 K. The mesopore volumes recorded under these two conditions were in good agreement with each other. A larger amount of Ar molecules had access to the micropores of the MFI-type zeolite. In terms of surface area determination, the NLDFT method conducted in the presence of Ar and N_2 could not be used to determine the micropore and mesopore surface areas, as the values largely overestimated the total surface areas determined by the BET method (Table 2, Tables S1-S7).

Table 2 Total surface area of hierarchical MFI-type zeolites.

Hierarchical MFI	S_{BET}-N_2[a] m^2/g	S_{BET}-Ar[a] m^2/g	S_{NLDFT}-N_2 m^2/g	S_{NLDFT}-Ar m^2/g
Micelle-Templated ZSM-5	517	444	622	1108
ZSM-5 Nanosheet spheres	491	422	622	889
ZSM-5 Nanosheet powder	440	404	268	644
Silicalite-1 Nanosheet spheres	372	367	553	890
Desilicated ZSM-5	446	438	620	1454
Silicalite-1 Nanocrystals	444	466	742	1175
ZSM-5 Nanocrystals	382	393	687	1408

[a]S_{BET}-N_2 calculated with σ_{N2} = 0.162 nm^2; S_{BET}-Ar calculated with σ_{Ar} = 0.142 nm^2

As an example, for the hierarchical ZSM-5 characterized by the presence of an aggregation of closely packed nanocrystals (50-100 nm), the BET surface area calculated from nitrogen isotherm recorded at 77 K was 380 m^2/g. This was in accordance with the geometrical nitrogen accessible surface area of the MFI structure [43] (367 and 379 m^2/g for a model of hard spheres and ovoids, respectively). The surface areas calculated by the NLDFT methods were 687 and 1408 m^2/g for N_2 and Ar, respectively (Table 2, Table S7). These results indicate a large overestimation of the surface areas calculated by the NLDFT method (proposed in the software of the instrument). All hierarchical MFI-type zeolites featured total surface areas determined by the BET equation (S_{BET}) in the range of 350-500 m^2/g (Table 1, Table 2, and Tables S1-S7).

The *t*-plots were analyzed for all hierarchical MFI-type zeolites (Figure 3, Figure 10, and Figure S1), with the first fit at low *t* values (3.2 < *t* < 4.2 Å) and a second fit at high *t* values (above 6 Å or above 10 Å for ZSM-5 and Silicalite-1 nanosheets, respectively). The mesopore plus external surface area ($S_{mes+ext}$) and the micropore volume (V_{mic}) were calculated based on the first fit at low *t* values. The total pore volumes (V_{tot}) were calculated at the end of the mesopore filling process. $S_{mes+ext}$ and V_{mic} were modified according to the corrections provided for ZSM-5 (Eq. 8-10) to obtain the corrected $S_{mes+ext*}$ and V_{mic*} values (see above). $S_{mes+ext*}$ was subtracted from S_{BET} to obtain the micropore surface areas (S_{mic}) (Eq. 11). V_{mic*} was subtracted from V_{tot} to obtain the mesopore volume (V_{mes}) (Eq. 12).

The micro-and mesopore volumes obtained from the corrected *t*-plot method were compared with the respective cumulative pore volumes obtained from the instrument software using the NLDFT method (Figure 11 and Figure S3, Tables S1-S7). The micropore and mesopore volumes calculated by the corrected *t*-plot methods are in good agreement with the results obtained using NLDFT in the presence of Ar at 87 K (method recommended by IUPAC [32] for pore volume

determination). Micelle-templated ZSM-5 and ZSM-5 nanosheet spheres present the maximum mesopore volume (approximately 0.25 mL/g) and the minimum micropore volume (approximately 0.12 mL/g). The other hierarchical MFI-type zeolites are characterized by a micropore volume of approximately 0.17 mL/g (as expected for pure ZSM-5) and varying mesopore volumes (0.12 mL/g for the ZSM-5 nanosheet powder, 0.15 mL/g for the Silicalite-1 nanosheet spheres, 0.03 mL/g for the desilicated ZSM-5 system, and null for nanocrystals of ZSM-5 and Silicalite-1). The coherence between the two methods (corrected *t*-plot method based on the N_2 isotherms recorded at 77K and the NLDFT analysis method based on the Ar isotherms recorded at 87K) was observed at ±0.03 mL/g.

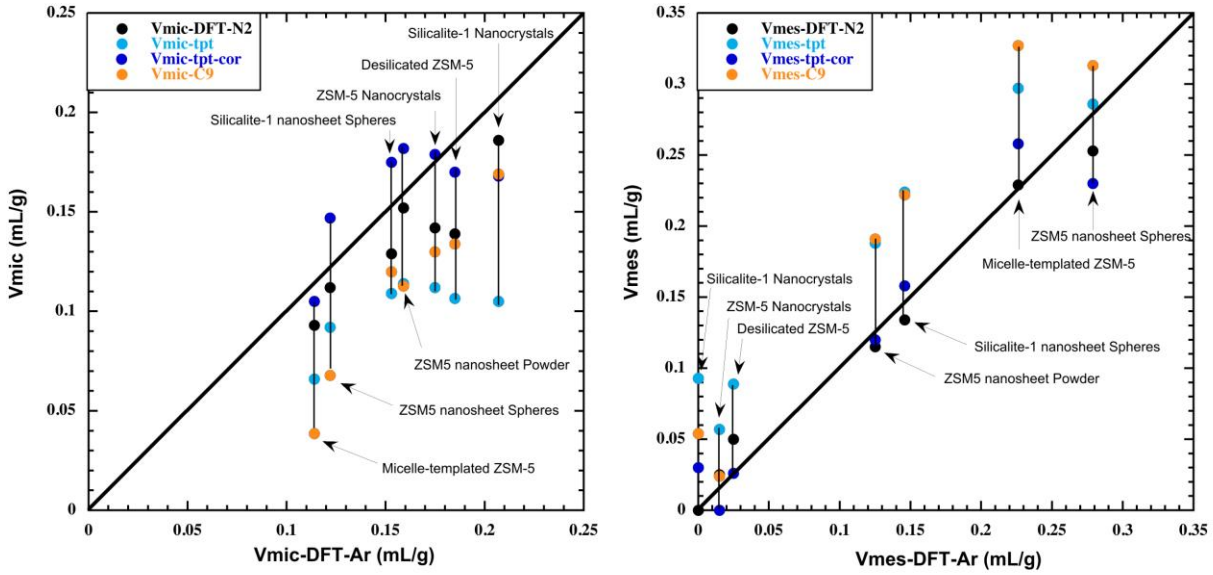

Figure 11 Comparison of (left) micropore and (right) mesopore volumes obtained by the different methods: *t*-plot, corrected *t*-plot, pre-adsorption of *n*-nonane followed by N_2 adsorption at 77 K, NLDFT based on the N_2 isotherm at 77 K (comparison was made with the volumes determined using the NLDFT method based on the Ar isotherm recorded at 87 K) for the different hierarchical MFI-type zeolites.

The *n*-nonane pre-adsorption method was used for the analysis of the different hierarchical MFI-type zeolites. Following the pre-adsorption of *n*-nonane, the N_2 isotherms recorded at 77 K can be used to directly visualize the mesoporous part of the hierarchical ZSM-5 (Figure 9) system. The isotherms can be analyzed to directly determine the mesopore volumes (V_{mes}) at the relative pressure where all mesopores are filled-up. The micropore volumes (V_{mic}) were calculated by the difference at p/p_0 = 0.5 of the pore volumes of the isotherms before and after *n*-nonane pre-adsorption (Tables S1-S7). These volumes were compared to the volumes obtained using the NLDFT methods and the *t*-plot analysis methods (Figure 11). The micropore volumes determined by *n*-nonane pre-adsorption method were lower than the volumes determined by the NLDFT method using Ar at 87 K (Figure 11). However, the volumes were comparable to the volumes determined following the NLDFT method using N_2 at 77 K (Figure S4). The exceptions consisted of 3 samples characterized by the presence of thin zeolite domains (2 nm) as micelle-templated ZSM-5 and ZSM-5 nanosheet sphere and powder, for which the micropore volumes were

underestimated (range: from -0.04 to -0.05 mL/g). This suggests that for these hierarchical ZSM-5 zeolites, a little amount of *n*-nonane evaporates from the mouth of the micropores during the outgassing step. This results in the underestimation of the micropore volume and overestimation of the mesopore volumes when the *n*-nonane pre-adsorption method is used. This was confirmed by the results obtained from the *t*-plot analysis of the samples filled with *n*-nonane. The results revealed a low micropore volume (0.014-0.018 mL/g), which potentially reflects the surface roughness (attributable to the micropore mouth openings) and not the intracrystalline micropores. It is noteworthy that the latter is not observed for silicalite-1 nanosheet spheres. This can be attributed to the strong interaction between *n*-nonane and the hydrophobic surface of this zeolite. Although desilicated ZSM-5 is characterized by a nitrogen isotherm that is similar to the one of ZSM-5 nanosheets powder (Figure 9), the evaporation of *n*-nonane was not observed. This indicated that in this catalyst, the zeolite domains were larger than 2 nm. The hysteresis loops recorded before and after the pre-adsorption of *n*-nonane were similar. This revealed that the embedded large mesopores (>20 nm) were connected to the exterior of the crystals via small mesopores (diameter: <5 nm) and not through the micropores of the zeolite system.

The corrected *t*-plot and the n-nonane pre-adsorption methods can be efficiently used for the determination of the surface areas. These methods are better than the NLDFT-based methods as the NLDFT-based methods overestimate the surface areas (compared to the BET surface areas) (Table 2, Tables S1-S7). For the *n*-nonane pre-adsorption method, the mesopore plus external surface area ($S_{mes+ext}$) was directly obtained by calculating the BET surface area of the N_2 isotherm post *n*-nonane pre-adsorption. The micropore surface area (S_{mic}) was calculated by determining the difference between the BET surface areas recorded before and after the pre-adsorption of *n*-nonane. Micelle-templated ZSM-5 and ZSM-5 nanosheet spheres were characterized by the maximum mesopore plus external surface areas (200-300 m^2/g) and the minimum micropore surface areas (200-250 m^2/g). The other hierarchical MFI-type zeolites are characterized by high micropore surface areas (300-350 m^2/g) and low mesopore plus external surface areas at approximately 100 m^2/g (Figure 12). Similar surface area results were obtained using the *n*-nonane pre-adsorption method and the corrected *t*-plot analysis method. The exceptions were the 3 samples characterized by the presence of thin zeolite domains (2 nm) as micelle-templated ZSM-5 and ZSM-5 nanosheet spheres and powder. For these cases, the micropore surface areas were underestimated, and the mesopore plus external surface areas were overestimated by the *n*-nonane preadsorption method. As explained above, this can be potentially attributed to the evaporation of *n*-nonane during the process of outgassing the samples.

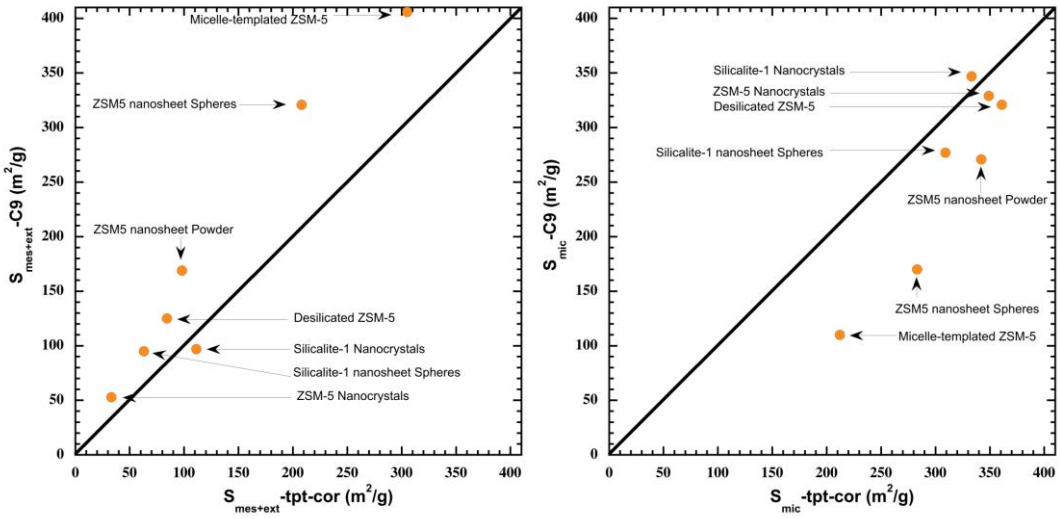

Figure 12 (left) Mesopore plus external surface areas and (right) micropore surface areas determined following the *n*-nonane pre-adsorption method. The results were compared with the results obtained using the corrected *t*-plot method for hierarchical MFI-type zeolites. Error is ±10 m^2/g for both methods.

4. Conclusions

Various hierarchical MFI-type zeolites (obtained following the process of desilication, via micelle-templating, and as nanosheets or nanocrystals) were analyzed following the corrected *t*-plot and the *n*-nonane pre-adsorption methods. The results were compared to the results obtained using the NLDFT methods performed with N_2 at 77 K and Ar at 87 K. The later is the most recommended method for studying hierarchical zeolites. The NLDFT methods cannot be efficiently used to determine the surface areas as values larger than that of the BET surface areas (i.e., the total surface area) were obtained. Micropore volumes obtained using the NLDFT method in the presence of N_2 at 77 K were underestimated in comparison to the values obtained using Ar at 87 K. However, comparable mesopore volumes were obtained. Micro-and mesopore volumes obtained following the corrected *t*-plot method were in good agreement with the volumes obtained using the NLDFT method performed with Ar at 87 K. Micro-and mesopore volumes obtained following the *n*-nonane pre-adsorption method agreed well with the volumes obtained using the NLDFT method performed with N_2 at 77 K. The exceptions were the hierarchical ZSM-5 systems characterized by the presence of thin zeolite domains (2 nm) as the micelle-templated ZSM-5 and nanosheet ZSM-5 systems. For these systems, the micropore volumes were underestimated due to small amount of *n*-nonane evaporated from the mouth of the micropores, and mesopore volumes were consequently overestimated. The corrected *t*-plot method and *n*-nonane pre-adsorption method could be used for the determination of the surface areas. However, the *n*-nonane pre-adsorption method could not be used to analyze the hierarchical ZSM-5 zeolites characterized by the presence of thin zeolite domains, resulting in the overestimation of the mesopore surface area and underestimation of the micropore surface area. The *n*-nonane pre-adsorption method is only valid for zeolites characterized by the presence of narrow ultramicropores (0.6 nm <) as MFI and for the large domain of zeolites (> 100 nm). The corrected

t-plot method can be used to evaluate the micropore and mesopore volumes and micropore and mesopore plus external surface areas of all kinds of hierarchical MFI-type zeolite catalysts.

Author Contributions

Cyril Vaulot, Habiba Nouali, Benedicte Lebeau, T. Jean Daou synthesized some of the hierarchical MFI and performed isotherms of Ar at 87 K and N_2 at 77 K for all hierarchical MFI and applied the NLDFT method to the isotherms. Lucie Desmurs synthesized the hierarchical MFI by micelle-templating and Al-MCM-41 and performed N_2 isotherms at 77 K and t-plot analysis. Isabelle Batonneau-Gener and Alexander Sachse synthesized some of the hierarchical MFI and performed the *n*-nonane preadsorption method for all the hierarchical MFI. Vasile Hulea and Claudia Cammarano supervised Lucie Desmurs work. Anne Galarneau supervised Lucie Desmurs work, performed *t*-plot analysis, made the comparison of the different methods of analysis and she wrote the manuscript. Alexander Sachse, Isabelle Batonneau-Gener, Jean Daou, Vasile Hulea, Claudia Cammarano revised the final manuscript.

Funding

The PhD work of Lucie Desmurs was funded by a “Contrat doctoral” of ENSCM, France.

Competing Interests

The authors declare no competing financial interest.

Additional Materials

The following additional materials are uploaded at the page of this paper.

1. Figure S1: Analysis of *t*-plots of hierarchical MFI-type zeolites indicating the range of the first fit (blue dashed lines) and the starting point (red vertical dashed line) of the second fit corresponding to (red horizontal dashed line) the “total” pore volume (micropore + mesopore volumes).
2. Figure S2: NLDFT-based cumulative pore volume for hierarchical MFI-type zeolites obtained using Ar at 87 K and N_2 at 77 K: (left) from 0 to 40 nm and (right) from 0 to 10 nm.
3. Figure S3: (left) Micropore volumes and (right) mesopore volumes determined following the corrected *t*-plot method from the N_2 adsorption isotherm recorded at 77 K. Comparisons were made with the NLDFT-based cumulative pore volume obtained by analyzing the Ar adsorption isotherm recorded at 87 K for the hierarchical MFI-type zeolites.
4. Figure S4: (left) Micropore volumes and (right) mesopore volumes determined following the *n*-nonane pre-adsorption method. The volumes were compared with the NLDFT-based cumulative pore volumes obtained by analyzing the N_2 adsorption isotherm at 77 K recorded for the hierarchical MFI-type zeolites.
5. Table S1: Porosity characterization of Sample 1: Micelle-templated Na-ZSM-5 (NaOH/Si = 0.55) (Si/Al = 15).
6. Table S2: Porosity characterization of Sample 2: Spheres (50 μm) of ZSM-5 nanosheets (Si/Al = 41), nanosheets thickness 2 nm.

7. Table S3: Porosity characterization of Sample 3: Powder of H,Na-ZSM-5 nanosheets (Si/Al = 45, nanosheet thickness: 2 nm).

8. Table S4: Porosity characterization of Sample 4: Spheres (20 μm) of Silicalite-1 nanosheets (nanosheet thickness: 3 nm).

9. Table S5: Porosity characterization of Sample 5: Desilicated ZSM-5 (HM02) (Si/Al = 40).

10. Table S6: Porosity characterization of Sample 6: Silicalite-1 Nanocrystals (nanocrystals diameter: 200 nm).

11. Table S7: Porosity characterization of Sample 7: ZSM-5 nanocrystals (Si/Al = 23); Diameter of nanocrystals: 50--150 nm.

References

1. Weitkamp J, Puppe L. Catalysis and zeolites: Fundamentals and applications. New York: Springer Science & Business Media; 1999.
2. Tanabea K, Hölderich WF. Industrial application of solid acid-base catalysts. Appl Catal A Gen. 1999; 181: 399-434.
3. Pérez-Ramírez J, Christensen CH, Egeblad K, Christensen CH, Groen JC. Hierarchical zeolites: Enhanced utilisation of microporous crystals in catalysis by advances in materials design. Chem Soc Rev. 2008; 37: 2530-2542.
4. Prech J, Pizzaro P, Serrano DP, Cejka J. From 3D to 2D zeolite catalytic materials. Chem Soc Rev. 2018; 47: 8263-8306.
5. Ivanova II, Knyazeva EE. Micro-mesoporous materials obtained by zeolite recrystallization: Synthesis, characterization and catalytic applications. Chem Soc Rev. 2013; 42: 3671-3688.
6. Kasyanov IA, Maerle AA, Ivanova II, Zaikovskii VI. Towards understanding of the mechanism of stepwise zeolite recrystallization into micro/mesoporous materials. J Mater Chem A. 2014; 2: 16978-16988.
7. Goto Y, Fukushima Y, Ratu P, Imada Y, Kubota Y, Sugi Y, et al. Mesoporous material from zeolite. J Porous Mater. 2002; 9: 43-48.
8. Ivanova II, Kasyanov IA, Maerle AA, Zaikovskii VI. Mechanistic study of zeolites recrystallization into micro-mesoporous materials. Microporous Mesoporous Mater. 2014; 189: 163-172.
9. Sachse A, Grau-Atienza A, Jardim EO, Linares N, Thommes M, Garcia-Martinez J. Development of intracrystalline mesoporosity through surfactant-templating. Cryst Growth Des. 2017; 17: 4289-4305.
10. Na K, Jo C, Kim J, Cho K, Jung J, Seo Y, et al. Directing zeolites structures into hierarchically nanoporous architectures. Science. 2011; 333: 328-332.
11. El Hanache L, Lebeau B, Nouali H, Toufaily J, Hamieh T, Daou TJ. Performance of surfactant-modified *BEA-type zeolite nanosponges for the removal of nitrate in contamined water: Effect of the external surface. J Hazard Mater. 2019; 364: 206-217.
12. Mehlhorn D, Rodriguez J, Cacciaguera T, Andrei RD, Cammarano C, Guenneau F, et al. Revelation on the complex nature of mesoporous FAU-Y zeolites. Langmuir. 2018; 34: 11414-11423.

13. El Hanache L, Sundermann L, Lebeau B, Toufaily J, Hamieh T, Daou TJ. Surfactant-modified MFI-type nanozeolites: Super-adsorbents for nitrate removal from contaminated water. Microporous Mesoporous Mater. 2019; 283: 1-13.
14. Huve J, Daou TJ, Nouali H, Patarin J, Ryzhikov A. The effect of nanostructures on high pressure intrusion-extrusion of water and electrolyte solutions in hierarchical nanoboxes of silicalite-1. New J Chem. 2020; 44: 273-281.
15. Choi M, Na K, Kim J, Sakamoto Y, Terasaki O, Ryoo R. Stable single-unit-cell nanosheets of zeolite MFI as active and long-lived catalysts. Nature. 2009; 461: 246-249.
16. Suarez N, Perez-Pariente J, Mondragon F, Moreno A. Generation of hierarchical porosity in beta zeolite by post-synthesis treatment with cetyltrimethylammonium cationic surfactant under alkaline conditions. Microporous Mesoporous Mater. 2019; 280: 144-150.
17. Al-Eid M, Ding L, Saleem Q, Badairy H, Sitepu H, Al-Maki A. A facile method to synthesize hierarchical nano-sized zeolite beta. Microporous Mesoporous Mater. 2019; 279: 99-106.
18. Mukti RR, Kamimura Y, Chaikittisilp W, Hirahara H, Shimojima A, Ogura M, et al. Hierarchically porous ZSM-5 synthesized by nonionic- and cationic-templating routes and their catalytic activity in liquid-phase esterification. ITB J Sci. 2011; 43A: 59-72.
19. Hartmann M, Machoke AG, Schweiger W. Catalytic test reactions for the evaluation of hierarchical zeolites. Chem Soc Rev. 2016; 45: 3313-3330.
20. Ivanova II, Kuznetsov AS, Yuschenko VV, Knyazeva EE. Design of composite micro/mesoporous molecular sieve catalysts. Pure Appl Chem. 2004; 76: 1647-1658.
21. Gackowski M, Datka J. Acid properties of hierarchical zeolites Y. Molecules. 2020; 25: 1044-1068.
22. Chawla A, Linares N, Rimer JD, Garcia-Martinez J. Time-resolved dynamics of intracrystalline mesoporosity generation in USY zeolite. Chem Mater. 2019; 31: 5005-5013.
23. Choi M, Na K, Ryoo R. The synthesis of a hierarchically porous BEA zeolite via pseudomorphic crystallization. Chem Comm. 2009. Doi: 10.1039/B905087F.
24. Srivasta R, Choi M, Ryoo R. Mesoporous materials with zeolite framework: Remarkable effect of the hierarchical structure for retardation of catalyst deactivation. Chem Comm. 2006. Doi: 10.1039/B612116K.
25. Al-Ani A, Haslam JJC, Mordvinova NE, Lebedev OI, Vicente A, Fernandez C, et al. Synthesis of nanostructured catalysts by surfactant-templating of large-pore zeolites. Nanoscale Adv. 2019; 1: 2029-2039.
26. Li K, Valla J, Garcia-Martinez J. Realizing the commercial potential of hierarchical zeolites: New opportunities in catalytic cracking. ChemCatChem. 2014; 6: 46-66.
27. Garcia-Martinez J, Xiao C, Cychosz KA, Li K, Wan W, Zou X, et al. Evidence of intracrystalline mesostructured porosity in zeolites by advanced gas sorption, electron tomography and rotation electron diffraction. ChemCatChem. 2014; 6: 3110-3115.
28. Vaugon L, Finiels A, Cacciaguera T, Hulea V, Galarneau A, Aquino C, et al. Impact of pore architecture on the hydroconversion of long chain alkanes over micro and mesoporous catalysts. Pet Chem. 2020; 60: 479-489.
29. Kazakov MO, Nadeina KA, Danilova IG, Dik PP, Klimov OV, Pereyma VY, et al. Hydrocracking of vacuum gas oil over NiMo/γ-Al_2O_3: Effect of mesoporosity introduced by zeolite Y recrystallization. Catal Today. 2018; 305: 117-125.

30. Kazakov MO, Nadeina KA, Danilova IG, Dik PP, Klimov OV, Pereyma VY, et al. Influence of USY zeolite recrystallization on physicochemical properties and catalytic performance of NiMo/USY-Al_2O_3 hydrocracking catalysts. Catal Today. 2019; 329: 108-115.
31. Landers J, Gor GY, Neimark AV. Density functional theory methods for characterization of porous materials. Colloids Surf A Physicochem Eng Asp. 2013; 437: 3-32.
32. Thommes M, Kaneko K, Neimark A, Olivier JP, Rodriguez-Reinoso F, Rouquerol J, et al. Physisorption of gases, with special reference to the evaluation of surface area and pore size distribution (IUPAC technical report). Pure Appl Chem. 2015; 87: 1051-1069.
33. Serrano DP, Aguado J, Morales G, Rodriguez JM, Peral A, Thommes M, et al. Molecular and meso- and macroscopic properties of hierarchical nanocrystalline ZSM-5 zeolite prepared by seed silanization. Chem Mater. 2009; 21: 641-654.
34. Li HC, Sakamoto Y, Liu Z, Ohsuna T, Terasaki O, Thommes M, et al. Mesoporous silicalite-1 zeolite crystals with unique pore shapes analogous to the morphology. Microporous Mesoporous Mater. 2007; 106: 174-179.
35. Thommes M, Mitchell S, Perez-Ramirez J. Surface and pore structure assessment of hierarchical MFI zeolites by advanced water and argon sorption studies. J Phys Chem C. 2012; 116: 18816-18823.
36. Cychosz KA, Guillet-Nicolas R, García-Martínez J, Thommes M. Recent advances in the textural characterization of hierarchically structured nanoporous materials. Chem Soc Rev. 2017; 46: 389-414.
37. Buttersack C, Mollmer J, Hofmann J, Glaser R. Determination of micropore volume and external surface of zeolites. Microporous Mesoporous Mater. 2016; 236: 63-70.
38. Villemot F, Galarneau A, Coasne B. Adsorption-based characterization of hierarchical metal-organic frameworks. Adsorption. 2014; 20: 349-357.
39. Villemot F, Galarneau A, Coasne B. Adsorption and dynamics in hierarchical metal organic frameworks. J Phys Chem C. 2014; 118: 7423-7433.
40. Coasne B, Galarneau A, Gerardin C, Fajula F, Villemot F. Molecular simulation of adsorption and transport in hierarchical porous materials. Langmuir. 2013; 29: 7864-7875.
41. Galarneau A, Villemot F, Rodriguez J, Fajula F, Coasne B. Validity of the t-plot method to assess microporosity in hierarchical micro/mesoporous materials. Langmuir. 2014; 30: 13266-13274.
42. Galarneau A, Mehlhorn D, Guenneau F, Coasne B, Villemot F, Minoux D, et al. Specific surface area determination for microporous/mesoporous materials: the case of mesoporous FAU-Y. Langmuir. 2018; 34: 14134-14142.
43. Desmurs L, Galarneau A, Cammarano C, Hulea V, Vaulot C, Nouali H, et al. Determination of microporous and mesoporous surface areas and volumes of mesoporous zeolites by corrected t-plot analysis. ChemNanoMat. 2022; 8:e202200051 (pp: 1-13).
44. Batonneau-Gener I, Sachse A. Determination of the exact microporous volume and BET surface area in hierarchical ZSM-5. J Phys Chem C. 2019; 123: 4235-4242.
45. Moukahhal K, Daou TJ, Josien L, Nouali H, Toufaily J, Hamieh T, et al. Hierarchical ZSM-5 beads composed of zeolite nanosheets obtained by pseudomorphic transformation. Microporous Mesoporous Mater. 2019; 288: 109565.

46. Moukahhal K, Lebeau B, Josien L, Galarneau A, Toufaily J, Hamieh T, et al. Synthesis of hierarchical zeolites with morphology control: Plain and hollow spherical beads of silicalite-1 nanosheets. Molecules. 2020; 25: 2563-2578.
47. Rouquerol F, Rouquerol J, Imelik B. Validité de la loi BET dans le cas de l'adsorption d'azote, d'argon et de butane sur des adsorbants poreux. Bull Soc Chim France. 1964. pp.635-639.
48. Rouquerol J, Llewellyn P, Rouquerol F. Is the BET equation applicable to microporous adsorbents? Stud Surf Sci Catal. 2007; 160: 49-56.
49. Bae YS, Yazaydin AO, Snurr RQ. Evaluation of the BET method for determining surface areas of MOFs and zeolites that contain ultra-micropores. Langmuir. 2010; 26: 5475-5483.
50. Gomez-Gualdron DA, Moghadam PZ, Hupp JT, Farha OM, Snurr RQ. On the application of consistency criteria to calculate BET areas of micro- and mesoporous metal-organic frameworks. J Am Chem Soc. 2016; 138: 215-224.
51. Broekhoff JC, De Boer JH. Studies on pore systems in catalysts: XIII. Pore distributions from the desorption branch of a nitrogen sorption isotherm in the case of cylindrical pores B. Applications. J Catal. 1968; 10: 377-390.
52. Galarneau A, Desplantier D, Dutartre R, Di Renzo F. Micelle-templated silicates as a test bed for methods of mesopore size evaluation. Microporous Mesoporous Mater. 1999; 27: 297-308.
53. Neimark AV, Ravikovitch PI. Capillary condensation in MMS and pore structure characterization. Microporous Mesoporous Mater. 2001; 44: 697-707.
54. Gregg SJ, Langford JF. Evaluation of microporosity, with special reference to a carbon black. Trans Faraday Soc. 1969; 65: 1394-1400.
55. Grillet Y, Llewellyn PL, Kenny MB, Rouquerol F, Rouquerol J. Evaluation of the n-nonane preadsorption method with a well characterized model adsorbent: Silicalite-1. Pure Appl Chem. 1993; 65: 2157−2167.
56. Thommes M, Cychosz KA. Physical adsorption characterization of nanoporous materials: Progress and challenges. Adsorption. 2014; 20: 233-250.
57. Lou F, Zhang A, Zhang G, Ren L, Guo X, Song C. Enhanced kinetics for CO_2 sorption in amine-functionalized mesoporous silica nanosphere with inverted cone-shaped pore structure. Appl Energy. 2020; 264: 114637.
58. Galarneau A, Calin N, Iapichella J, Barrande M, Denoyel R, Coasne B, et al. Optimization of the properties of macroporous chromatography silica supports through surface roughness control. Chem Mater. 2009; 21: 1884-1892.

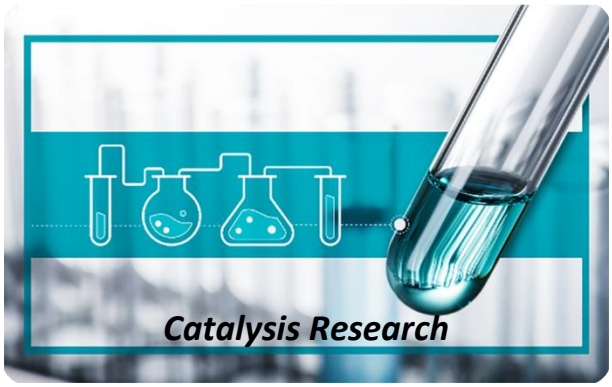

Enjoy *Catalysis Research* by:

1. Submitting a manuscript
2. Joining in volunteer reviewer bank
3. Joining Editorial Board
4. Guest editing a special issue

For more details, please visit:
http://www.lidsen.com/journals/cr